nature chemical biology

BRIEF COMMUNICATION

https://doi.org/10.1038/s41589-018-0186-1

Riboregulated toehold-gated gRNA for programmable CRISPR–Cas9 function

Ka-Hei Siu and Wilfred Chen*

Predictable control over gene expression is essential to elicit desired synthetic cellular phenotypes. Although CRISPR–Cas9 offers a simple RNA-guided method for targeted transcriptional control, it lacks the ability to integrate endogenous cellular information for efficient signal processing. Here, we present a new class of riboregulators termed toehold-gated gRNA (thgRNA) by integrating toehold riboswitches into sgRNA scaffolds, and demonstrate their programmability for multiplexed regulation in *Escherichia coli* with minimal cross-talks.

Orthogonal control over gene expression is critical for constructing biological circuits that can reliably redirect cellular functions into new phenotypes[1,2]. Previous efforts relied on the use of ligand-responsive transcription factors (LRTFs), which must be meticulously customized for each target of interest[3,4]. Their limited number and orthogonality further hinder the construction of more complex, robust circuits in living cells. An alternative is to use RNA-based regulators[5,6]. However, the dearth of well-characterized RNA sensor–actuator pairs and modest dynamic range limit their utility[7,8]. Ideally, hybrid protein–RNA devices combining the unique advantages of both systems can be created.

The CRISPR–Cas9 system offers a unique RNA-guided approach for DNA targeting[9,10], and nuclease-null Cas9 (dCas9) has been repurposed as a transcriptional regulator[11]. Switchable guide RNAs (gRNAs) have been created using either a ligand-induced conformation switch or cleaving motif to uncage the spacer-blocking region[12,13]. Though these strategies facilitate conditional activation of Cas9 functions by externally delivered ligands or selected intracellular proteins[13,14], they lack the ability to implement autonomous control based on endogenous cellular information. Inspired by the simplicity of toehold-mediated strand displacement[15] and the success of new riboregulators termed toehold switches[16], we designed conditional gRNA structures termed toehold-gated gRNA (thgRNA; Fig. 1a) and demonstrated their utility for providing orthogonal gene regulation using synthetic and endogenous RNA triggers.

The thgRNA is initially sequestered, with a stem-loop structure that renders the spacer unavailable for target binding (Fig. 1a). A structural change is induced by binding the trigger strand to the toehold region preceding the 5′-end of the stem-loop, initiating branch migration into the stem-loop region and exposing the spacer for target binding (Fig. 1a). We first screened our designs computationally by using NUPACK[17] to minimize unintended secondary structures and to maximize interactions between the trigger and thgRNA. We selected five candidates that target the same target sequence, A, and synthesized the variants A1–A5 for further testing (Fig. 1b; Supplementary Fig. 1; Supplementary Table 1).

The initial characterization of thgRNAs exploited the native nuclease activity of Cas9 to cut its DNA target sequence (Fig. 1c; Supplementary Fig. 2). Of the five variants, most exhibited positive correlations between trigger concentrations and cleavage activities (Fig. 1c; Supplementary Fig. 2b), suggesting that these thgRNA variants were activated through binding with the trigger strand A*. Only variant A5 displayed substantial background activity without the trigger. We speculate that the short stem structure on A5 may be unstable, and thus spontaneously unwinds to expose the spacer for DNA binding.

To evaluate the kinetics of activation, we employed a FRET-based beacon assay that detects dissociation of a fluorescently labeled strand from a quencher strand upon Cas9 binding (Supplementary Fig. 3a)[18]. Background fluorescence remained low for all variants except A5, consistent with the DNA cleavage assay. Binding of Cas9 to the DNA target was restored for all variants upon addition of the trigger stand A*. With the exception of A4, the rise in fluorescence in the presence of A* was comparable to that in the unmodified sgRNA (Supplementary Fig. 3b), suggesting that neither 5′-extension nor hybridization of the trigger strand compromised the target binding capabilities of the Cas9–thgRNA complex. Together with the DNA cleavage assay, we demonstrated a framework for conditional activation of Cas9 activity using switchable gRNA structures modulated by toehold-mediated strand displacement.

Using the design principle for A1, we generated three additional thgRNAs, B, C, and D, targeting three separate orthogonal DNA targets (Supplementary Fig. 1) and characterized each using the beacon assay (Supplementary Fig. 3c). The toehold and branch migration sequences of A and B were entirely artificial, whereas those of C and D were designed to hybridize with two endogenous small RNA (sRNA) sequences (OxyS and RyhB). The need to pair with native sequences imposed sequence constraints on these thgRNAs, resulting in a more sequestered conformation for thgRNA D; this may have caused the decreased kinetics and lowered fluorescence signal observed, similar to that in thgRNA A4 (Supplementary Fig. 3). Nonetheless, thgRNAs A1, B, C, and D all displayed negligible background activities and $>75\%$ increase in fluorescence signals relative to the unmodified sgRNAs, suggesting that the basic thgRNA design can be readily adapted for both native and synthetic sequences. Moreover, all thgRNAs exhibited excellent orthogonality and provided selective activation of the corresponding beacon even in a multiplexed setting (Supplementary Fig. 4).

We next tested the use of thgRNAs as intracellular RNA-responsive switches to regulate CRISPR interference (CRISPRi) in *E. coli* (Fig. 2a). Co-expression of dCas9 and the corresponding sgRNA resulted in complete repression of Nluc (Supplementary Fig. 5). In contrast, co-expression of dCas9 and thgRNA had little impact on Nluc expression, indicating in vivo blocking of dCas9 binding. Induction of trigger RNA expression by IPTG reduced the Nluc level by >10-fold for samples expressing both thgRNA and dCas9, but had no impact for the control expressing dCas9 alone (Fig. 2b, A1). Although a similar ΔthgRNA without the flanking

Department of Chemical and Biomolecular Engineering, University of Delaware, Newark, DE, USA. *e-mail: wilfred@udel.edu

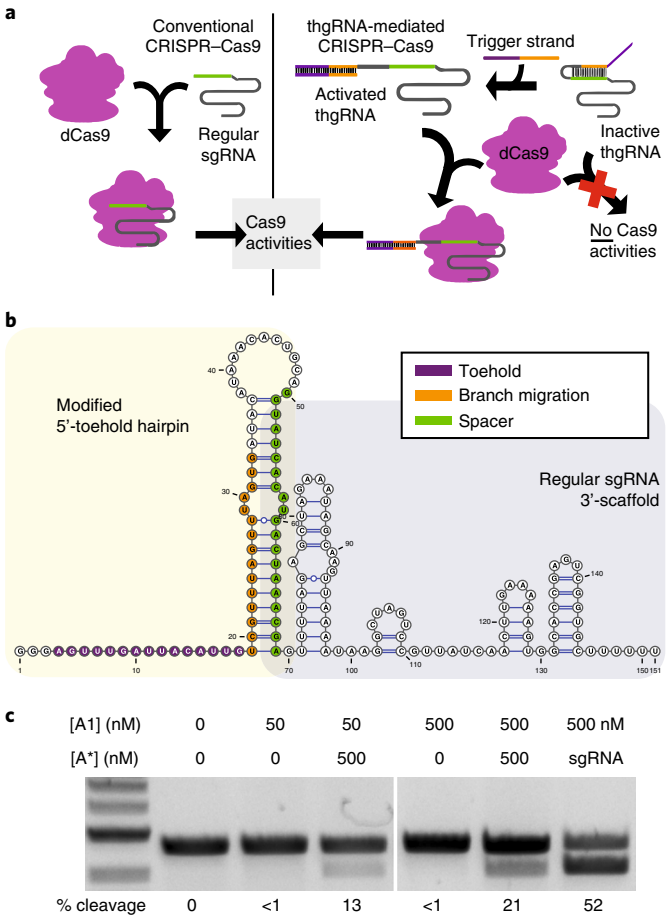

Fig. 1 | Design and screening of toehold-gated guide RNAs (thgRNAs). **a**, Schematic representation of thgRNA-based activation of CRISPR–Cas9 functions. **b**, The minimum free energy (MFE) structure of thgRNA A1 at 37 °C as predicted by the NUPACK algorithm. **c**, In vitro activation of Cas9 cleavage by toehold-mediated strand displacement. Both thgRNA A1 and trigger A* must be present with the Cas9 nuclease to cleave linearized plasmid DNA. Gels display representative results from 1 of 3 independent experiments.

toehold sequence was also effective in blocking dCas9 activation, the addition of IPTG had little effect on Nluc expression. This result highlights the importance of the toehold sequence and confirms opening of the stem-loop by strand displacement. Collectively, these results demonstrate the successful intracellularly implementation of toehold-gated dCas9 riboregulators.

To test in vivo orthogonality, we assembled the expression cassettes for dCas9, thgRNAs, and the Nluc reporter into a single plasmid[19] (Supplementary Fig. 6; Supplementary Table 2) and placed the different trigger strands under the control of either an inducible pL*lac*O-1 or pL*tet*O-1 promoter[20] using a separate plasmid. Addition of either isopropyl β-D-1-thiogalactopyranoside (IPTG) or anhydrotetracycline (ATc) induces expression of the trigger strand, resulting in transcriptional repression. Although the extent of Nluc repression (~4- to 12-fold) varied among the four thgRNAs, CRISPRi was activated by the cognate trigger strands in all cases (Fig. 2b). Limited cross-talks were observed, except for ~50% repression between thgRNA A1 and trigger C*. This is likely caused by unintended interactions between A1 and C*, which were also observed in the beacon assay. To mitigate these limitations, it may be possible to manipulate the blocking stem-loop structures to further increase the thermodynamic driving force for strand displacement and Cas9 activation as described by previous works on similar toehold-based RNA switches[16,21].

We next evaluated the kinetics and sensitivity of the CRISPRi activation using thgRNA B. Repressions of both Nluc transcripts and activity were observed as early as 1 h post-induction, with a maximum repression of ~ 10-fold detected after 4 h (Supplementary Fig. 7a). Additionally, CRISPRi could be modulated by different dosages of ATc, with maximum repression detected at a modest 1 ng/mL (Supplementary Fig. 7b), ten-fold lower than the maximum expression attainable by the pL*tet*O-1 promoter[20]. Because the number of DNA targets is limited by the plasmid copy number, only small numbers of trigger strands are needed to activate Cas9 binding for all available target sites. These results demonstrated that the switchable activation of thgRNAs is fast and sensitive.

To establish the possibility of deploying thgRNAs for multiplexed regulation, we replaced Nluc with mCherry and BFP for targets B and D, respectively, and constructed a plasmid expressing the three reporters, thgRNAs, and dCas9 (Supplementary Table 2). Significant repression was detected only when the appropriate triggers were induced with no significant cross-talks observed (Fig. 2c). Given the high selectivity and orthogonality of using thgRNAs for multiplexed regulation, this strategy can be adapted to construct even more complex genetic circuit designs.

Another important feature is incorporation of endogenous RNAs as trigger strands[16,22]. We designed thgRNAs C and D to be responsive to sRNAs, OxyS and RyhB, respectively[23,24] (Supplementary Fig. 8a). Expression of RyhB is induced by iron deficiency through the addition of 2,2′-bipyridyl. A dose-dependent repression of Nluc expression was observed only by paring thgRNA D with the corresponding reporter cassette (Fig. 3a). Similarly, repression was observed with co-expression of full-length OxyS sRNA induced by artificial promoter pL*tet*O-1 (Supplementary Fig. 8b). We further demonstrated the generality of the approach for different endogenous sequences by designing six additional thgRNAs targeting two native sRNAs (97-bp MicF and 227-bp SgrS) and three regions of the full-length mCherry mRNA (Supplementary Fig. 1; Supplementary Table 1). Though not all new designs were as effective as C and D, most exhibited some degree of intracellular response, including those designed for the longer SgrS (F) and mCherry (G2) transcripts that elicited > 70% repression (Fig. 3b; Supplementary Fig. 9). Importantly, no notable decrease in mCherry fluorescence was observed for any samples that exploited mCherry mRNA as the trigger, indicating that translation is not inhibited significantly even after binding to the thgRNAs (Fig. 3c). These results highlight the feasibility of designing thgRNAs that are responsive to a range of native RNA sequences, including full-length mRNA, without compromising the cellular functions of endogenous strands.

To expand the use of thgRNAs as a tool for inducible gene knockout[25], we investigated whether thgRNA activation can be used to induce plasmid loss by nuclease active Cas9. We introduced two plasmids (containing either an AmpR or KanR selection marker) into *E. coli* and induced the expression of trigger B*, selectively cleaving the plasmid containing AmpR. After 4 h induction, we observed ~ 60% reduction in the number of colonies for the induced sample relative to the uninduced sample and controls (Supplementary Fig. 10). The ability to provide conditional gene knockout in *E. coli* paves the way for inducible genome editing in eukaryotic systems based on differential RNA expression.

Our thgRNAs offer a simple 'plug and play' design for conditional activation of CRISPR-based systems by a virtually unlimited set of RNA triggers using highly predictable toehold-mediated strand displacement reactions. Because activation is enabled by sequence-specific unblocking of the spacer, this design offers orthogonality, low cross-talk with unrelated endogenous information, and high sequence versatility. The flexibility to exploit endogenous RNAs to regulate gene expression provides a simple interface between native

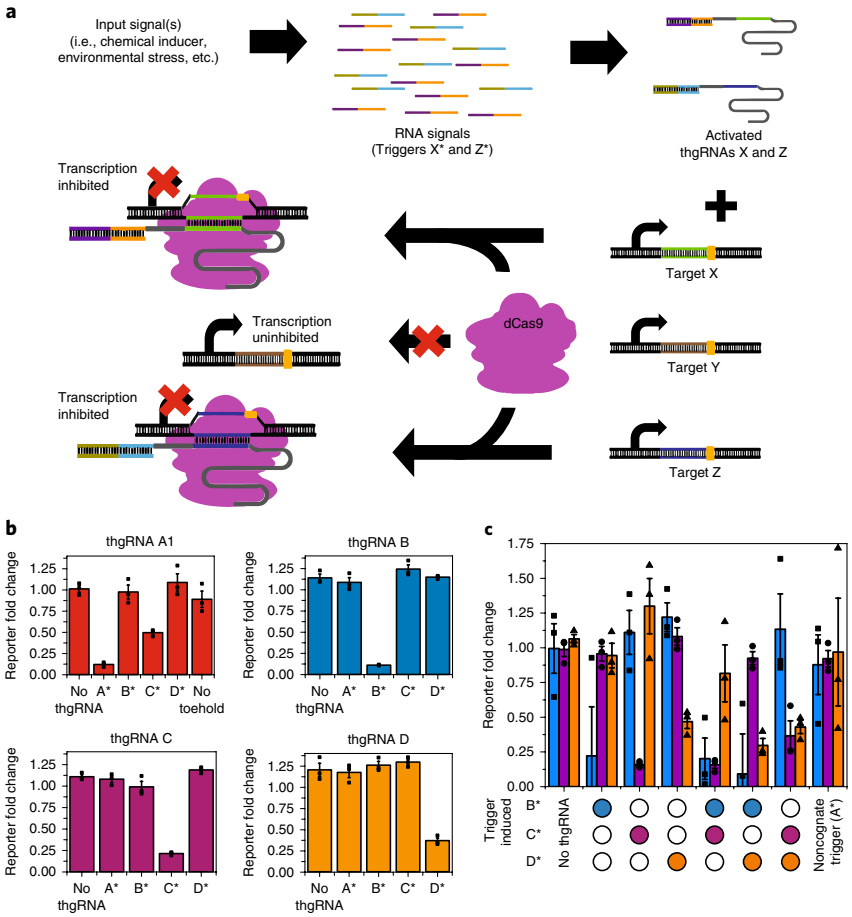

Fig. 2 | thgRNAs can be selectively activated intracellularly by induced expression of cognate trigger RNAs. a, RNA-responsive thgRNA could be applied to restore Cas9 functions to specific targets inside the cells, regardless of the origin of the RNA trigger sequence. **b**, Induced repression of the Nluc reporter by different combinations of thgRNAs and triggers. Reporter fold change is defined as the Nluc luminescence observed with induction of the indicated trigger on the *x* axis over the Nluc luminescence observed without induction of trigger. **c**, Multiplexed activation of thgRNA–dCas9-mediated repression by induced expression of specific trigger strands indicated as filled circles on the *x* axis corresponding to the color coding in **b**. The open circles indicate no expression of the corresponding trigger strand. Normalized fold change is defined as the reporter signal observed with induction of the indicated trigger(s) over the signal observed without induction of trigger(s). Values are mean ± s.e.m. with $n = 3$ from different transformants in three independent experiments in all plots.

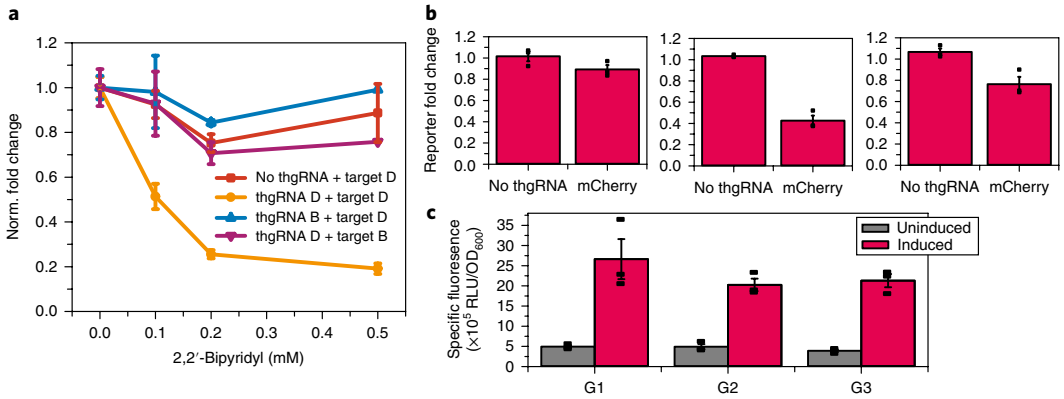

Fig. 3 | thgRNA can be activated specifically by endogenous RNAs. a, Induced repression of the Nluc reporter using the native iron-responsive RyhB sRNA as the trigger. Repression of Nluc by addition of increasing concentrations of 2,2′-bipyridyl is observed only when thgRNA D and target D are both present. **b**, mCherry mRNA can be used as a trigger to activate thgRNA. Three thgRNA (G1–G3) designed to hybridize to three distinct regions of mCherry mRNA were screened for inducible Nluc repression. The graphs correspond to G1, G2, G3, from left to right. Of the three variants, G2 displayed the highest level of repression at ~60%. **c**, Observed mCherry fluorescence exhibited no correlation with degree of induced repression by activated thgRNA, suggesting that the use of the mRNA as a trigger strand does not significantly inhibit its ability to be translated by cellular translational machinery. $P > 0.05$; two-sided Student's *t*-tests were performed between induced samples. Values are mean ± s.e.m. with $n = 3$ from different transformants in three independent experiments in all plots.

signals and synthetic transcriptional outputs, bypassing the often tedious process of screening large libraries currently needed to create specific LRTFs or riboregulators.

Theoretically, our thgRNA design allows us to execute complex multi-input logic operations by stacking several RNAs into a single trigger, similarly to the multi-input activation of toehold switches recently reported[21]. However, we anticipate the need for further optimizations of thgRNA and trigger designs to account for additional secondary structures and interactions with Cas9 protein. These complications may introduce kinetic and thermodynamic barriers that may prevent efficient activation of thgRNAs. Investigations on multi-input designs are underway.

Online content

Any methods, additional references, Nature Research reporting summaries, source data, statements of data availability and associated accession codes are available at https://doi.org/10.1038/s41589-018-0186-1.

Received: 17 January 2018; Accepted: 1 November 2018;
Published online: 10 December 2018

References

1. Khalil, A. S. & Collins, J. J. *Nat. Rev. Genet.* **11**, 367–379 (2010).
2. Lim, W. A. *Nat. Rev. Mol. Cell Biol.* **11**, 393–403 (2010).
3. Taylor, N. D. et al. *Nat. Methods* **13**, 177–183 (2016).
4. Tang, S. Y. & Cirino, P. C. *Angew. Chem. Int. Ed. Engl.* **50**, 1084–1086 (2011).
5. Serganov, A. & Nudler, E. *Cell* **152**, 17–24 (2013).
6. Chappell, J., Watters, K. E., Takahashi, M. K. & Lucks, J. B. *Curr. Opin. Chem. Biol.* **28**, 47–56 (2015).
7. Callura, J. M., Cantor, C. R. & Collins, J. J. *Proc. Natl Acad. Sci. USA* **109**, 5850–5855 (2012).
8. Mutalik, V. K., Qi, L., Guimaraes, J. C., Lucks, J. B. & Arkin, A. P. *Nat. Chem. Biol.* **8**, 447–454 (2012).
9. Horvath, P. & Barrangou, R. *Science* **327**, 167–170 (2010).
10. Wiedenheft, B., Sternberg, S. H. & Doudna, J. A. *Nature* **482**, 331–338 (2012).
11. Qi, L. S. et al. *Cell* **152**, 1173–1183 (2013).
12. Tang, W., Hu, J. H. & Liu, D. R. *Nat. Commun.* **8**, 15939 (2017).
13. Liu, Y. et al. *Nat. Methods* **13**, 938–944 (2016).
14. Davis, K. M., Pattanayak, V., Thompson, D. B., Zuris, J. A. & Liu, D. R. *Nat. Chem. Biol.* **11**, 316–318 (2015).
15. Zhang, D. Y. & Winfree, E. *J. Am. Chem. Soc.* **131**, 17303–17314 (2009).
16. Green, A. A., Silver, P. A., Collins, J. J. & Yin, P. *Cell* **159**, 925–939 (2014).
17. Zadeh, J. N. et al. *J. Comput. Chem.* **32**, 170–173 (2011).
18. Mekler, V., Minakhin, L., Semenova, E., Kuznedelov, K. & Severinov, K. *Nucleic Acids Res.* **44**, 2837–2845 (2016).
19. Xu, P., Vansiri, A., Bhan, N. & Koffas, M. A. G. *ACS Synth. Biol.* **1**, 256–266 (2012).
20. Lutz, R. & Bujard, H. *Nucleic Acids Res.* **25**, 1203–1210 (1997).
21. Green, A. A. et al. *Nature* **548**, 117–121 (2017).
22. Groves, B. et al. *Nat. Nanotechnol.* **11**, 287–294 (2016).
23. Altuvia, S., Zhang, A., Argaman, L., Tiwari, A. & Storz, G. *EMBO J.* **17**, 6069–6075 (1998).
24. Massé, E., Escorcia, F. E. & Gottesman, S. *Genes Dev.* **17**, 2374–2383 (2003).
25. Ran, F. A. et al. *Nat. Protoc.* **8**, 2281–2308 (2013).

Acknowledgements

This work was supported by grants to W.C. from the National Science Foundation (MCB1615731 and MCB1817675). We thank D. Liu (Harvard University), T. Pederson (University of Massachusetts Medical School), and M. Koffas (Rensselaer Polytechnic Institute) for their generous gifts of plasmids as noted in the manuscript.

Author contributions

K-H.S. and W.C. conceived the project. K-H.S. designed experiments, performed the experiments, analyzed the data, and wrote the manuscript. W.C. designed experiments, analyzed the data, and wrote the manuscript. Both authors discussed the results and commented on the manuscript.

Competing interests

The authors declare no competing interests.

Additional information

Supplementary information is available for this paper at https://doi.org/10.1038/s41589-018-0186-1.

Reprints and permissions information is available at www.nature.com/reprints.

Correspondence and requests for materials should be addressed to W.C.

Publisher's note: Springer Nature remains neutral with regard to jurisdictional claims in published maps and institutional affiliations.

Methods

Design and computational screening of thgRNA variants. NUPACK algorithm[17] was used to model all thgRNA variants before any experimental work (Supplementary Fig. 1). Except for thgRNAs A2–5, which were designed and screened to test the limits of thgRNA structures (length of toehold, stem-loop, etc.), the toehold, branch migration, and spacer regions of all other thgRNAs were screened and modified to follow the general design of thgRNA A1, emulating rules outlined by Green et al[16]. (Supplementary Fig. 1a), wherever possible. Stable secondary structures in the toehold region were avoided in all instances where artificial trigger sequences were used. Pair-wise complexes between thgRNAs and trigger strands were also modeled by the same algorithm to predict formation of hybridized dimers, as intended or otherwise. The full sequences of all thgRNAs, trigger strands, and DNA targets tested are reported in Supplementary Table 1.

When endogenous sRNAs were intended to be used as trigger strands, previous literature[23,24] was referenced wherever available to check the computationally predicted structures modeled by NUPACK. The artificial trigger strands C* and D* were designed to mimic single-stranded regions of the sRNA or regions where hybridization with the native targets were experimentally observed by previous works. Both the artificial triggers and endogenous sequences were further modeled for hybridization with the thgRNAs. All thgRNAs A, B, C, and D and any variants characterized in subsequent experimental studies were predicted to form stable complexes with their cognate trigger strands.

Strains used and plasmids construction. All strains and plasmids used in this study are listed in Supplementary Table 2.

Plasmids used for in vitro DNA cleavage assays containing targets A, B, C, or D were constructed based on high-copy-number backbone pUC19 and transformed into NEB 5α *E. coli* strain (New England BioLabs, Inc., Ipswich, MA, USA) to ensure high plasmid yields. Expression construct for Cas9 protein was obtained as a gift from D. Liu (Addgene plasmid # 62374) and transformed into BL21-Gold(DE3) cells for expression. dCas9 gene was amplified from pHAGE-TO-dCas9–3XmCherry (Addgene plasmid # 64108), a gift from T. Pederson.

The unmodified ePathBrick[19] vector, pETM6, was a generous gift from M. Koffas and was used as the initial backbone for our intracellular expression constructs. Briefly, we created a new BioBrick-compatible vector capable of constitutive expression by substituting the synthetic constitutive promoter J23115p in place of the *lac*-inducible T7-*lac*O promoter and constructed a set of expression constructs for each sgRNA/thgRNA, target and downstream reporter and Cas9 or dCas9; this allowed us to rapidly combine sets of expression cassettes into a single plasmid that can be easily co-transformed into *E. coli* with a trigger plasmid (See Supplementary Fig. 6 for detailed scheme). The trigger plasmids were constructed by Gibson assembly and standard subcloning techniques.

DNA cleavage and Förster resonance energy transfer (FRET)-based beacon assays. Plasmids containing DNA targets A, B, C, and D were constructed as described above. Target DNA were harvested from NEB 5α cells transformed with the relevant plasmids using Zyppy miniprep kit according to the vendor's instructions (Zymo Research, Irvine, CA, USA) and linearized by restriction digests using NotI enzyme before cleavage assays. Cas9 proteins were expressed from *E. coli* and purified as described by previous study[26]. All RNAs were transcribed in vitro using HiScribe T7 Quick High Yield RNA Synthesis Kit (New England BioLabs, Inc., Ipswich, MA, USA) and purified by standard phenol-chloroform extraction and ethanol precipitation. RNA purity and quality was analyzed by spectrophotometry on a NanoDrop 2000 UV-Vis spectrophotometer (Thermo Fisher Scientific, Inc., Waltham, MA, USA) and denaturing urea PAGE electrophoresis using 5% polyacrylamide gels containing 8 M urea[27]. Unmodified and fluorophore- or quencher-labeled oligonucleotides were synthesized and purified by commercial vendor (Integrated DNA Technologies, Inc., Coralville, IA, USA).

For DNA cleavage assay, thgRNA and DNA mimetic trigger strand or unmodified sgRNA were first incubated at 37 °C for 15 min. Reactions containing linearized plasmid targets, purified Cas9 protein, and pre-incubated thgRNA/trigger strand or sgRNA were then mixed with final concentrations as denoted into cleavage reaction buffer (100 mM NaCl, 50 mM Tris–HCl, 10 mM $MgCl_2$, 100 μg/ml BSA, pH 7.9), and incubated at 37 °C for 1 h. Reaction products were then analyzed by electrophoresis on 1% agarose gel with ethidium bromide stains. Percent of cleavage was estimated by densitometry using ImageJ (NIH).

For FRET-based beacon assay, beacon complexes containing target A, B, C, or D were assembled by mixing the 5′-fluorophore-labeled target strand, the PAM-containing strand, and the 3′-quencher labeled strand to a final concentration of 2 μM in nuclease-free water, heated to 90 °C, and cooled to room temperature at a rate of 0.1 °C/s using a S1000 Thermal Cycler (Bio-Rad Laboratories, Inc., Hercules, CA, USA). All fluorescence measurements were carried out in binding buffer (20 mM Tris–HCl, 120 mM NaCl, 5% v/v glycerol, 0.1 mM DTT, 1 mM $MgCl_2$, 0.02% v/v Tween 20, pH 7.9)[18] and measured using a Synergy H4 Hybrid microplate reader (BioTek Instruments, Inc., Winooski, VT, USA) at 25 °C. Final assay mixtures contained 5 nM assembled beacon complex, 50 nM Cas9 protein, 50 nM sgRNA or thgRNA, and varying concentrations of trigger strands as indicated. Excitation and emission wavelengths were tailored to the fluorophore used for each target (A: FAM, ex: 498 nm, em: 520 nm; B: TYE 563, ex: 545 nm, em: 565 nm; C: TEX 615, ex: 595 nm, em: 615 nm; D: TYE 665, ex: 64 5 nm, em: 665 nm). Pre-incubated thgRNA/trigger strand or sgRNA was added at $t = 0$ s, and measurements were taken every 6–30 s for the initial 600 s and every 30 s for the remainder of the assays.

Induced transcriptional repression by CRISPRi using artificial trigger strands. NEB 5α cells were transformed with a plasmid containing the constitutively expressed reporter, thgRNA, and dCas9 cassettes and a trigger plasmid containing either B*, C*, D*, or combinations thereof by heat shock. Successful transformants were picked from agar plates and grown in LB medium (10 g/L tryptone, 5 g/L yeast extract,10 g/L NaCl) supplemented with 100 μg/mL carbenicillin and 50 μg/mL kanamycin for ~ 10–12 h at 37 °C. The resulting cultures were used to inoculate subcultures at an initial OD ~ 0.03 and grown to OD ~ 1. Expression of the artificial trigger strands were then induced by inoculating fresh LB media containing the corresponding inducers (500 mM IPTG, 10 ng/mL ATc, or both) at an initial OD ~ 0.03. These cultures were incubated at 37 °C for ~ 4–5 h, at which point mid-late exponential phase (OD ~ 1) would be reached, and samples were taken.

Cell samples were pelleted by centrifugation at 3,000 *g* for 5 min, washed twice with PBS (137 mM NaCl, 2.7 mM KCl, 10 mM Na_2HPO_4, 1.8 mM KH_2PO_4, pH 7.4), and resuspended to OD ~ 2 in PBS before measurements. Whole-cell luminescence were measured according to NanoGlo vendor's instructions (Promega Corporation, Madison, WI, USA) using a Synergy H4 Hybrid microplate reader. Whole-cell fluorescence were also measured with the microplate reader where needed. Analysis of luminescence and fluorescence data were completed using Origin software (OriginLab Corporation, Wellesley Hills, MA, USA).

Total RNA was extracted from samples using Direct-zol miniprep kit according to vendor's instructions (Zymo Research, Irvine, CA, USA). Transcript expression was then quantified using qPCR using Luna Universal qPCR Master Mix (New England BioLabs, Inc., Ipswich, MA, USA) according to the manufacturer's protocol. All samples were run in technical duplicate on a CFX96 Touch Real-Time PCR Detection System (Bio-Rad Laboratories, Hercules, CA, USA). All PCR primers were verified as being specific on the basis of melting curve analysis and were as follows: Nluc: 5′-GGTGTCCGTAACTCCGATCC-3′ and 5′-ATCCACAGGGTACACCACCT-3′; *ssrA*: 5′-TTAGGACGGGGATCAAGAGA-3′ and 5′-GCGTCCGAAATTCCTACATC-3′. Transcript levels of Nluc were calculated by subtracting housekeeping control (*ssrA*) cycle threshold (C_t) values from Nluc C_t values to normalize for total input, yielding ΔC_t levels. Relative transcript levels was computed as $2^{-\Delta Ct}$.

sRNA and mRNA induced repression. NEB 5α cells were transformed with a plasmid containing the expression cassettes for the reporter, thgRNA, and dCas9 and grown as described above. Full-length OxyS, MicF, SgrS sRNA and mCherry mRNA replaced artificial trigger sequence to activate their respective thgRNA. Induction of RyhB sRNA was achieved by addition of varying concentrations of 2,2′-bipyridyl as noted in Fig. 3a instead of IPTG or ATc as described above for induction under pL*lac*O-1 or pL*tet*O-1 promoters.

Induced plasmid loss. NEB 5α cells were transformed with a plasmid containing the expression cassettes for the reporter and thgRNA B as well as a compatible plasmid containing *tet*-inducible trigger B* and nuclease active Cas9 protein under constitutive promoter J23115. Transformed cells were grown, induced, and collected as described above. twofold serial dilutions of collected cells resuspended to initial $OD_{600} \sim 10^{-3}$ were prepared in PBS and 20 μL of each dilution spotted onto LB agar plates containing only kanamycin or both ampicillin and kanamycin as noted in Supplementary Fig. 10. Colonies forming units were visually counted and compared between the two plates to estimate the loss of ampicillin resistance, indicating loss of the corresponding plasmid containing Cas9 target and AmpR marker.

Statistics and reproducibility. All information on statistical methods and reproducibility is shown in the corresponding figure legends.

Reporting Summary. Further information on experimental design is available in the Nature Research Reporting Summary linked to this article.

Data availability

Sequences of all thgRNAs and trigger strands studied are included in the Supplementary Information. Additional data that support the findings of this study are available from the authors on reasonable request.

References

26. Gagnon, J. A. et al. *PLoS One* **9**, e98186 (2014).
27. Summer, H., Grämer, R. & Dröge, P. *J. Vis. Exp.* **32**, e1485 (2009).

nature research

Corresponding author(s): Wilfred Chen

Life Sciences Reporting Summary

Nature Research wishes to improve the reproducibility of the work that we publish. This form is intended for publication with all accepted life science papers and provides structure for consistency and transparency in reporting. Every life science submission will use this form; some list items might not apply to an individual manuscript, but all fields must be completed for clarity.

For further information on the points included in this form, see Reporting Life Sciences Research. For further information on Nature Research policies, including our data availability policy, see Authors & Referees and the Editorial Policy Checklist.

Please do not complete any field with "not applicable" or n/a. Refer to the help text for what text to use if an item is not relevant to your study.

For final submission: please carefully check your responses for accuracy; you will not be able to make changes later.

Experimental design

1. Sample size

   Describe how sample size was determined.

   No statistical method was used to predetermine the sample size. The sample size (n>=3 independent experiments) reported for all experiments were based on values commonly accepted in the literature that provide sufficient robustness. All sample sizes are described in the individual figure legends.

2. Data exclusions

   Describe any data exclusions.

   Exclusion criteria are not pre-established. Multiple independent transcriptional repression experiments are performed, with the occasional bacterial cultures (~10-20%) of E. coli transformed with multiple plasmids failing to grow (OD600<0.1 after 4-5hrs from initial OD600~0.03) during subculture in fresh media with antibiotics, suggesting the population no longer contains one or more of the plasmids encoding one or more of the required genes of interests. As such, these samples yield no meaningful results and are excluded from analysis.

3. Replication

   Describe the measures taken to verify the reproducibility of the experimental findings.

   All experiments were performed independently at least 3 times, excluding the outliers excluded as described above; all attempts at replications were successful otherwise.

4. Randomization

   Describe how samples/organisms/participants were allocated into experimental groups.

   The is not relevant to biochemical studies and samples were not randomized.

5. Blinding

   Describe whether the investigators were blinded to group allocation during data collection and/or analysis.

   The is not relevant to biochemical studies and the investigators were not blinded.

Note: all in vivo studies must report how sample size was determined and whether blinding and randomization were used.

6. Statistical parameters

For all figures and tables that use statistical methods, confirm that the following items are present in relevant figure legends (or in the Methods section if additional space is needed).

n/a	Confirmed
☐	☒ The exact sample size (*n*) for each experimental group/condition, given as a discrete number and unit of measurement (animals, litters, cultures, etc.)
☐	☒ A description of how samples were collected, noting whether measurements were taken from distinct samples or whether the same sample was measured repeatedly
☐	☒ A statement indicating how many times each experiment was replicated
☒	☐ The statistical test(s) used and whether they are one- or two-sided *Only common tests should be described solely by name; describe more complex techniques in the Methods section.*
☐	☒ A description of any assumptions or corrections, such as an adjustment for multiple comparisons
☐	☒ Test values indicating whether an effect is present *Provide confidence intervals or give results of significance tests (e.g. P values) as exact values whenever appropriate and with effect sizes noted.*
☐	☒ A clear description of statistics including central tendency (e.g. median, mean) and variation (e.g. standard deviation, interquartile range)
☐	☒ Clearly defined error bars in all relevant figure captions (with explicit mention of central tendency and variation)

See the web collection on statistics for biologists for further resources and guidance.

Software

Policy information about availability of computer code

7. Software

Describe the software used to analyze the data in this study.

NUPACK web application and source code are published by the NUPACK team and available to the public through http://www.nupack.org/. Data was analyzed in Origin 2015 Sr2.

For manuscripts utilizing custom algorithms or software that are central to the paper but not yet described in the published literature, software must be made available to editors and reviewers upon request. We strongly encourage code deposition in a community repository (e.g. GitHub). *Nature Methods* guidance for providing algorithms and software for publication provides further information on this topic.

Materials and reagents

Policy information about availability of materials

8. Materials availability

Indicate whether there are restrictions on availability of unique materials or if these materials are only available for distribution by a third party.

No unique materials were used.

9. Antibodies

Describe the antibodies used and how they were validated for use in the system under study (i.e. assay and species).

No antibodies were used.

10. Eukaryotic cell lines

a. State the source of each eukaryotic cell line used.

No eukaryotic cell lines were used.

b. Describe the method of cell line authentication used.

No eukaryotic cell lines were used.

c. Report whether the cell lines were tested for mycoplasma contamination.

No eukaryotic cell lines were used.

d. If any of the cell lines used are listed in the database of commonly misidentified cell lines maintained by ICLAC, provide a scientific rationale for their use.

No eukaryotic cell lines were used.

Animals and human research participants

Policy information about studies involving animals; when reporting animal research, follow the ARRIVE guidelines

11. Description of research animals

Provide all relevant details on animals and/or animal-derived materials used in the study.

No animals were used/

Policy information about studies involving human research participants

12. Description of human research participants

Describe the covariate-relevant population characteristics of the human research participants.	No human research participants were involved in the study.